International Research Journal of Engineering and Technology (IRJET) e-ISSN: 2395-0056
Volume: 08 Issue: 03 | Mar 2021 www.irjet.net p-ISSN: 2395-0072

DESIGN AND ANALYSIS OF GAS TURBINE BLADE USING CFD

B.Vincent[1], G. Abinicks Raja[2], S. Prince Antony Claret[3]

[1]Assistant Professor, Dept. of Mechanical Engineering, Vel Tech High Tech Dr.Rangarajan Dr.Sakunthala Engineering College, Chennai, Tamilnadu, India.
[2]Assistant Professor, Dept. of Aeronautical Engineering, Bharath Institute of Higher Education and Research, Chennai, Tamilnadu, India.
[3]Dept. of Mechanical Engineering, St.Joseph's College of Engineering, Chennai, Tamilnadu, India.

Abstract – *Gas turbines have an important role in electric power generation and are used in a variety of configurations. Turbine rotor blades are the most important components in a gas turbine power plant and are mainly affected due to static loads. Use of rib turbulators is an effective technique to enhance the rate of heat transfer to gas flow in the gas turbine blades which enhances its cooling by creating turbulence over the boundary of the wall. The heat transfer in turbulent boundary layer will be more when compared to the laminar boundary layer. In this work, Analysis Sharp ribs of sizes 3mm, 6mm & 9mm in rectangular channels are used, and the flow analysis is determined with the help of ANSYS15 .In this research the Reynolds number of the range of 10000 and 15000 are analyzed for various parameters like temperature and velocity. It is predicted that the ribs of different sizes will enhance the heat transfer rate and pressure drop in the rectangular channel section. Also the Temperature variations, Wall Heat Transfer Coefficient, Average Heat Transfer Coefficient, Friction factor, Velocity, Pressure drop of developed turbulent flow in rectangular channel of cross section 100*80*300mm are compared.*

Key Words: Rib Turbulators, Flow Analysis, Reynolds Number, Heat Transfer Rate, Pressure Drop, Friction factor.

1. INTRODUCTION

The gas turbine in its most common form is a rotary heat operating by means of series of processes consisting of air taken from the atmosphere, increase of gas temperature by constant pressure combustion of the fuel in the whole process being continuous. Gas turbine are used extensively for aircraft propulsion, land based power generation and industrial application. Thermal efficiency and power output of gas turbine increases with increasing turbine rotor inlet temperature. The current rotor inlet temperature level in advanced gas turbine is far above the melting point of the blade material. Therefore, along with high temperature development, sophisticated cooling scheme must be developed for continuous safe operation of gas turbine with high performance. The melting temperature of the turbine blades is the limitation considered here. So this melting temperature may affect the material of the turbine blade. In the compressor, the flow of the working fluid is compressed at first. It is then heated in the combustion chamber. Finally, it goes through the turbine. The turbine converts the energy of the gas into mechanical work. Therefore turbine blades should to be cooled. The blades are cooled by extracted air from the compressor of the engine. The cooling system must be designed in a way that the maximum blade surface temperature and temperature gradients during operation will be compatible with maximum blade thermal stress for the life of the design.

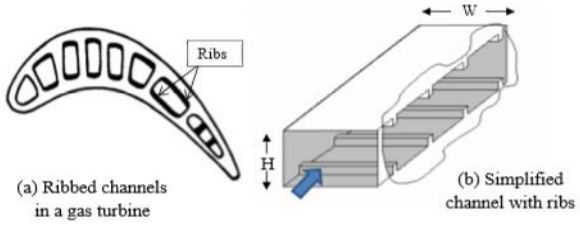

Fig-1: Rib turbulators in a gas turbine cooling channel

2. METHODOLOGY

Computational Fluid Dynamics (CFD) helps in our analysis of the rectangular channel with and without boot shaped ribs of different heights in a flow of Reynolds number 10000, 15000, 20000 and 30000. This analysis helps to simulate the internal cooling configurations in a gas turbine blade to understand the characteristics of the turbulent flow and heat transfer. Boot sectioned ribs of sizes 0 (smooth duct), 3, 6 and 9 mm were chosen to study the influence of the rib height on the overall performance of the channel. Computational analysis will be compared amongst each models and literature for best result. The advantage of using CFD is the availability of three dimensional flow field results as compared to single measured point experiment result, and it is useful in designing more efficient augmented heat transfer channels. CATIA V5R20 software was used for modeling and 'ANSYS' was used for the computational analysis.

2.1 Modelling and Analysis

The physical domain considered for the computational study is rectangular channel test section with or without

ribs. The length of the test channel is 300mm with outer cross-section breadth and height 110mm and 90mm. The thickness of the channel is 5mm.

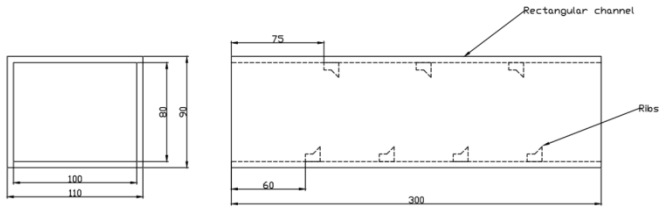

Fig-2: Two Dimensional Sectional View of the Model

It can be observed that four ribs were created at the bottom wall surface and as well as three ribs were created at the top surfaces.

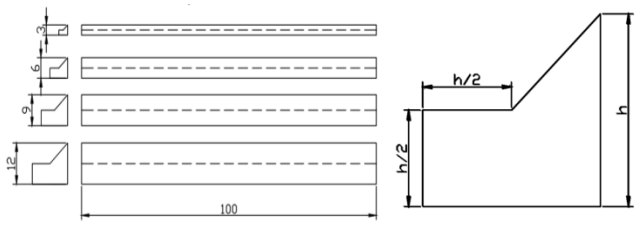

Fig-3: Two Dimensional View and proportion of the Ribs

First the Computational analysis was conducted in smooth rectangular channel with the aspect ratio of 1.25. The computations were then carried out for the channels with rib turbulators of different heights. The rib heights tested were 0, 3, 6, and 9mm. In a particular channel, all the ribs were made of same height. Each model is analyzed in fluid flow of Reynolds number 10000 and 15000. A constant heat flux of 3400 W/m^2 was maintained at the top and bottom surfaces of the test section. Air will be considered to enter the channel through a section such that air falls first on the shorter side of the rib faces. Since the channel exits are open to atmosphere, there is no restriction to the flow to provide any induced back pressure. Thus there is no possibility of the working fluid to get compressed. Also from the preliminary investigations and hand calculations, the velocity of the air flow inside the ducts were found for respective Reynolds numbers, which is very low considering subsonic Mach number. Hence the flow inside these ducts can be treated as incompressible.

2.2 Mesh Details

The mesh for the computational domain is made with tetrahedral cells, as the geometry is complex. The numerical grid contains a finer near wall and rib surfaces, with the first node placed at 0.1 mm and with a cell size growth factor of 1.1, normal to the wall.

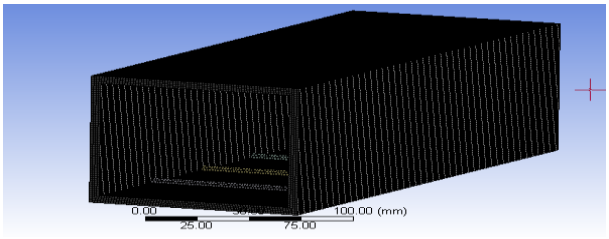

Fig-4: Meshed computational domain for the rectangular 3mm ribbed channel

SIMPLE algorithm is used for the process for coupling the pressure and velocity. The second order upwind differencing scheme is used for convective terms and for the turbulence quantities in order to enhance the numerical accuracy of the results. The grid independency test was carried out by measuring the temperature values along the top surface of 3mm ribs model.

2.3 Boundary Condition

The boundary conditions of the computational analysis are velocity inlet for the channel extended inlet whose value is deduced from the corresponding Reynolds number value and fluid properties of air. The air inlet temperature for the particular channel configuration is taken from the ambient conditions. The channel outer wall is specified with a constant heat flux value. The outlet of the flow domain has a constant static pressure value of '0'.

S.NO	Nodes	Elements	Max Face Size (mm)
1	438568	391628	2
2	681671	616932	1.7
3	1217510	1124222	1.4
4	1508286	1399930	1.3

Table -1: Grid Independency Test

2.4 Convergence Criteria

Based on scaled residuals for the equations of continuity, energy and turbulence quantities specific to the respective models the convergence criteria for the computational solutions are determined. Until the convergence criterions were met, every case is made to run. The iterations are continued for 1000 more iterations and stopped to achieve iterative convergence for cases where the convergence oscillates and cases where convergence was not achieved.

3. RESULTS AND DISCUSSIONS

The results from the computations carried out on the rectangular channels with and without ribs (smooth channel) are discussed below. The results are categorized according to the Reynolds numbers. Pressure variations, temperature variations and wall heat transfer coefficient are plotted along the surfaces of every rectangular channel with respective Reynolds number of 10000 and 15000.

The curves drawn for 3mm, 6mm and 9mm are compared with the curve drawn for smooth surface without rib model.

3.1 Temperature Contours

The temperature contours along the rectangular channel are displayed for smooth surface, 3mm ribbed, 6mm ribbed and 9mm ribbed channels for Reynolds numbers 10000 and 15000.

3.1.1 Reynolds Number 10000

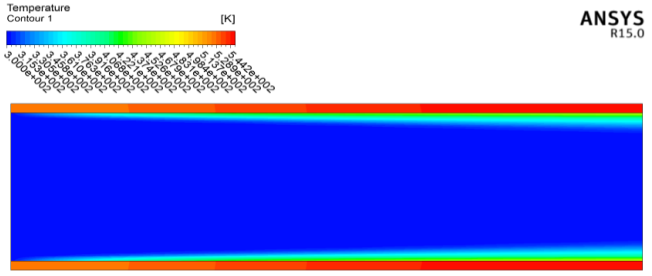

Fig-5: Temperature Contour in smooth channel

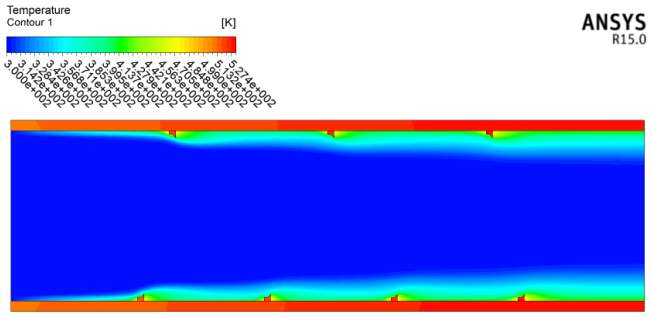

Fig-6: Temperature Contour in 3mm ribbed channel

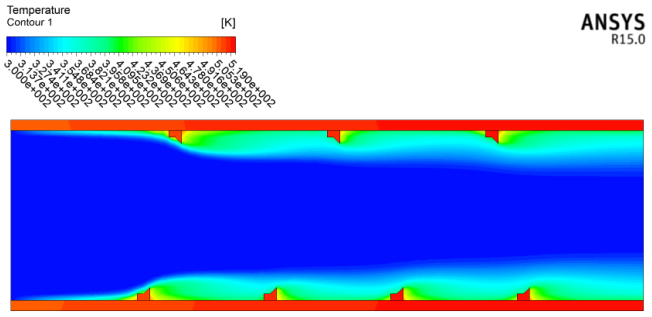

Fig-7: Temperature Contour in 6mm ribbed channel

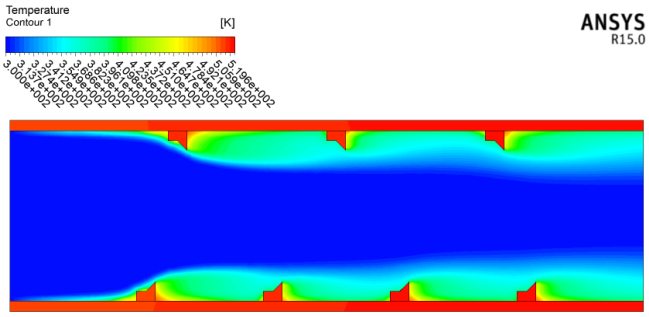

Fig-8: Temperature Contour in 9mm ribbed channel

3.1.2 Reynolds Number 15000

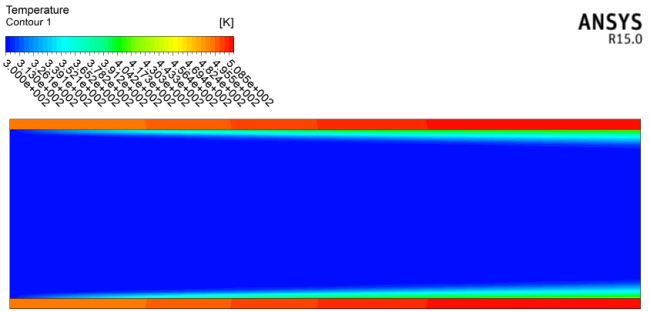

Fig-9: Temperature Contour in smooth channel

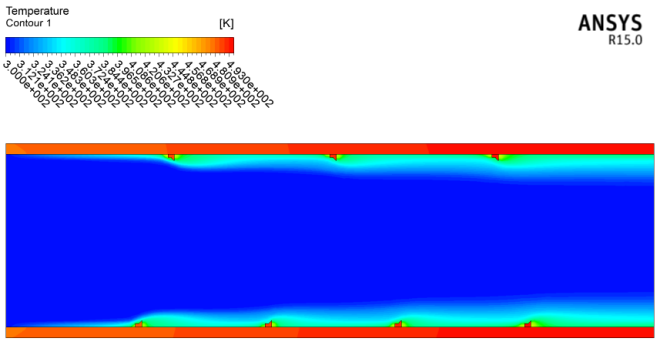

Fig-10: Temperature Contour in 3mm ribbed channel

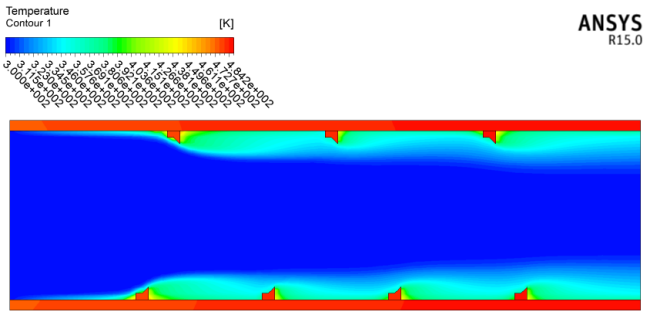

Fig-11: Temperature Contour in 6mm ribbed channel

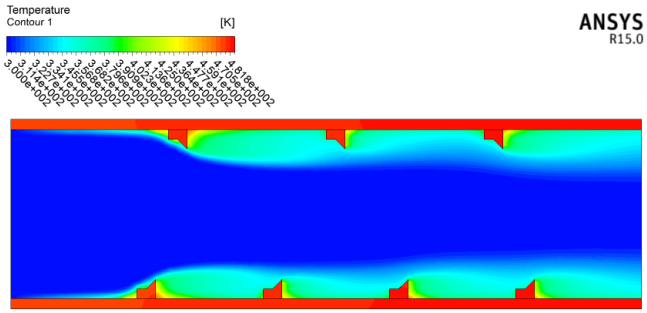

Fig-12: Temperature Contour in 9mm ribbed channel

3.2 Velocity Contours

The velocity along the channel are displayed for smooth surface, 3mm ribbed, 6mm ribbed and 9mm ribbed channels for Reynolds numbers 10000 and 15000.

3.2.1 Reynolds Number 10000

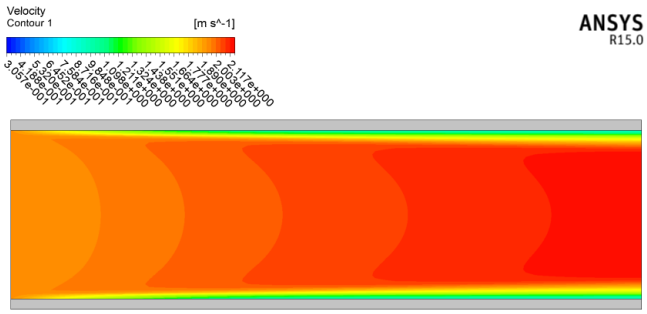

Fig-13: Velocity Contour in smooth channel

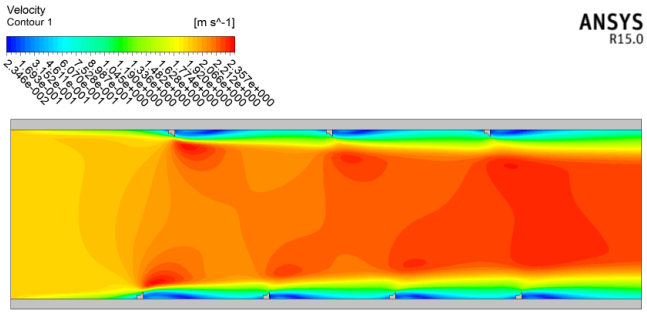

Fig-14: Velocity Contour in 3mm ribbed channel

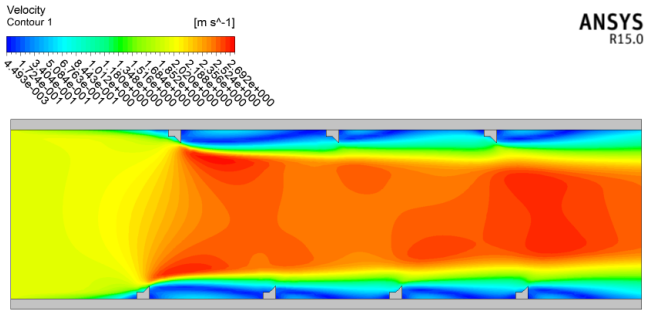

Fig-15: Velocity Contour in 6mm ribbed channel

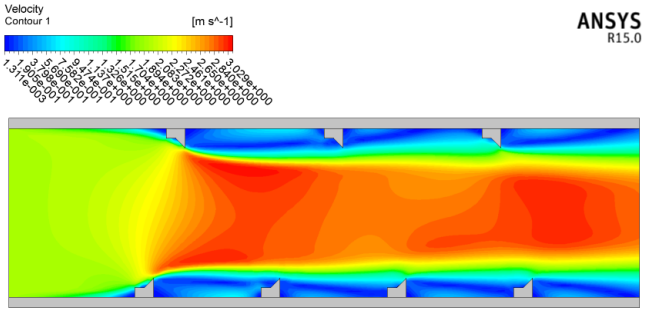

Fig-16: Velocity Contour in 9mm ribbed channel

3.2.2 Reynolds Number 15000

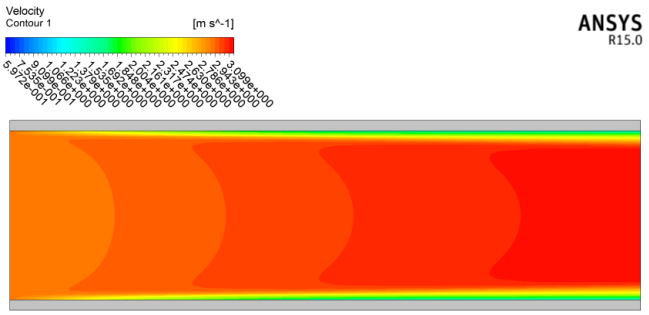

Fig-17: Velocity Contour in smooth channel

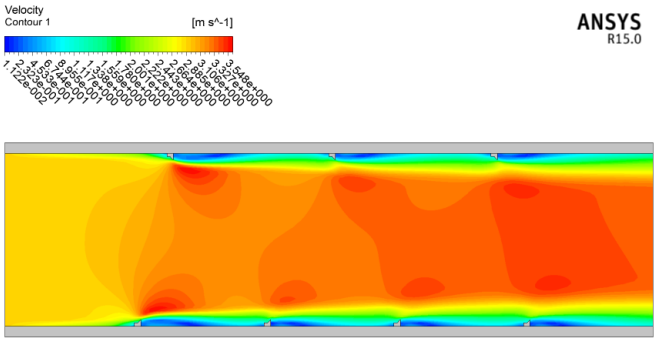

Fig-18: Velocity Contour in 3mm ribbed channel

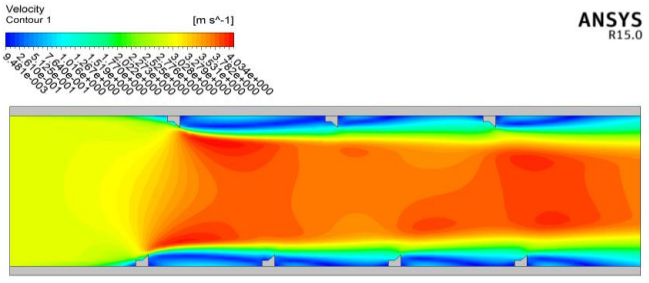

Fig-19: Velocity Contour in 6mm ribbed channel

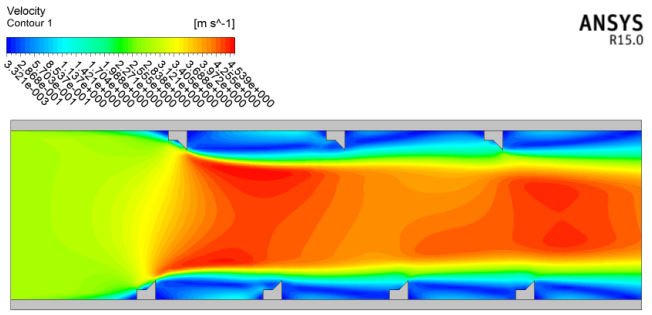

Fig-20: Velocity Contour in 9mm ribbed channel

3.3 Temperature Variations

Temperature variations along the top and bottom surface of every channel are depicted below.

3.3.1 Reynolds Number 10000

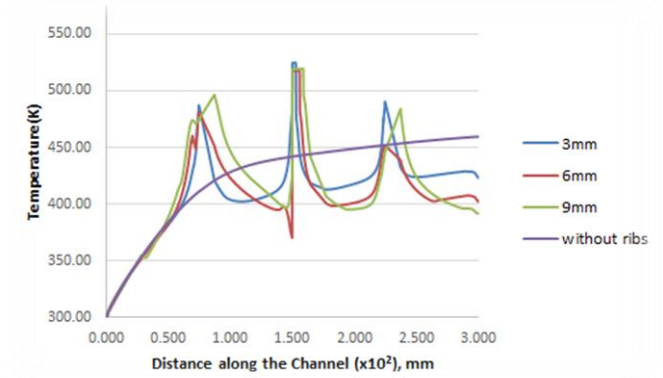

Chart -1: Temperature variations along Top Surface

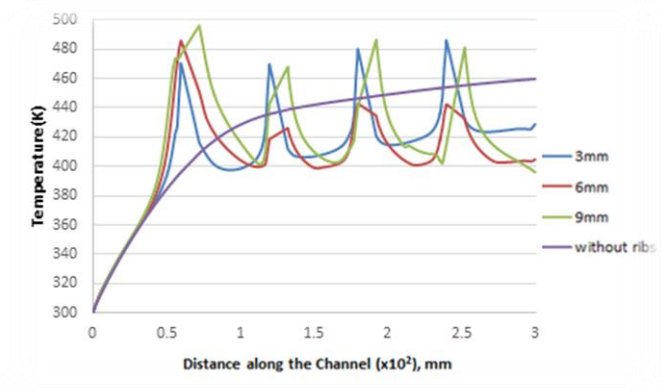

Chart -2: Temperature variations along Bottom Surface

3.3.1 Reynolds Number 15000

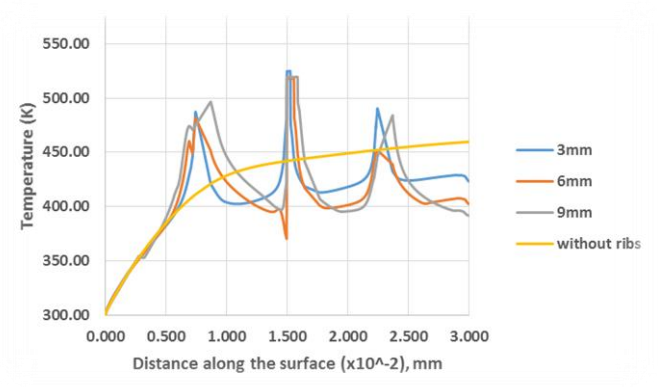

Chart -3: Temperature variations along Top Surface

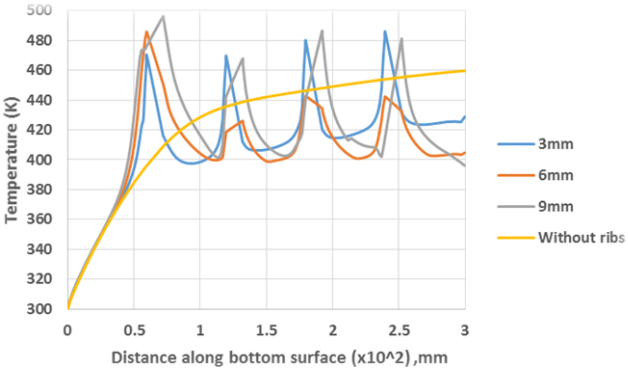

Chart -4: Temperature variations along Bottom Surface

3.4 Wall Heat Transfer Coefficient

3.4.1 Reynolds Number 10000

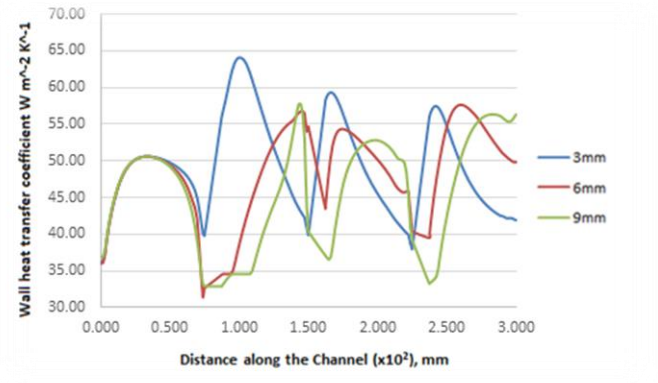

Chart -5: Wall Heat Transfer Coefficient along Top Surface

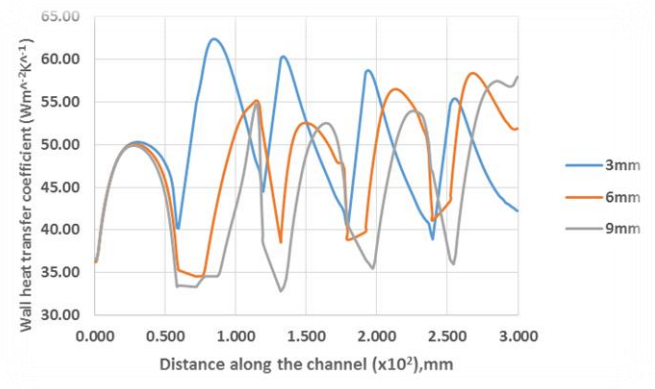

Chart -6: Wall Heat Transfer Coefficient along Bottom Surface

3.4.2 Reynolds Number 15000

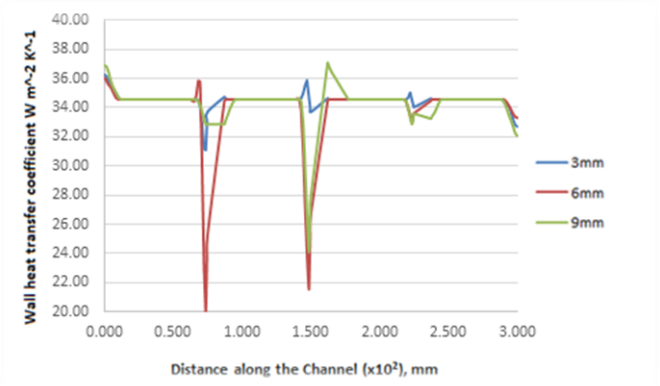

Chart -7: Wall Heat Transfer Coefficient along Top Surface

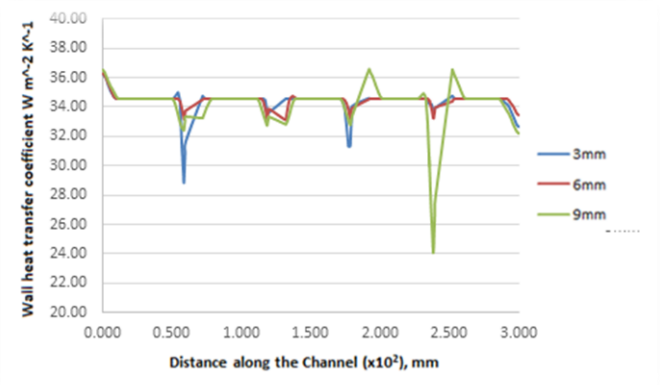

Chart -8: Wall Heat Transfer Coefficient along Bottom Surface

3.5 Average Temperature

3.5.1 Top Surface

Table -2: Average Temperature along Top Surface

Reynolds Number	Rib Type	Temperature (K)
10000	3mm	336.14
	6mm	335.28
	9mm	338.71
	Without Ribs	340.95
15000	3mm	407.25
	6mm	401.55
	9mm	408.70
	Without Ribs	422.82

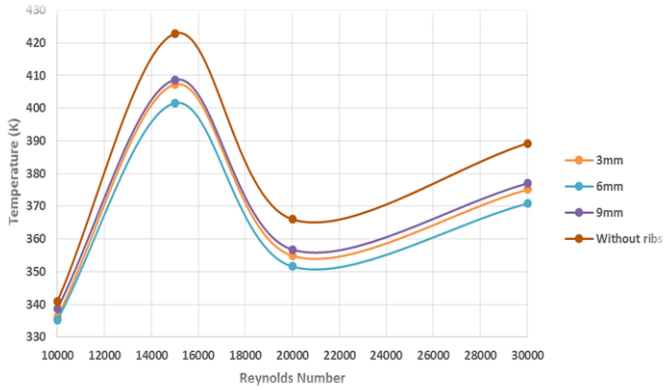

Chart -9: Temperature along Top Surface Vs Reynolds Number

3.5.2 Bottom Surface

Table -3: Average Temperature along Bottom Surface

Reynolds Number	Rib Type	Temperature (K)
10000	3mm	334.73
	6mm	333.94
	9mm	337.39
	Without Ribs	340.93
15000	3mm	403.35
	6mm	399.91
	9mm	408.99
	Without Ribs	422.60

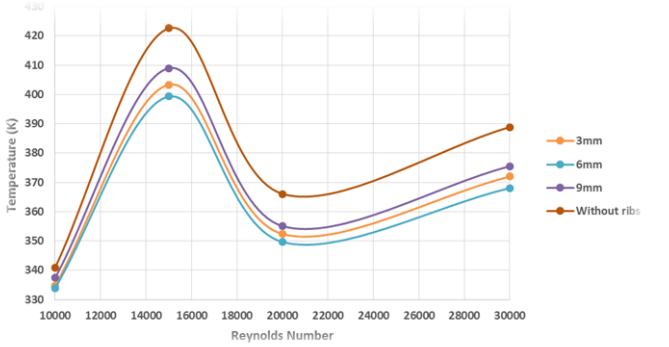

Chart -10: Temperature along Bottom Surface Vs Reynolds Number

3.6 Average Wall Heat Transfer Coefficient

3.6.1 Top Surface

Table -4: Average Wall Heat Transfer Coefficient along Top Surface

Reynolds Number	Rib Type	Average Wall Heat Transfer Coefficient (W m^-2K^-1)
10000	3mm	49.50
	6mm	49.18
	9mm	46.70
15000	3mm	34.54
	6mm	34.16
	9mm	34.34

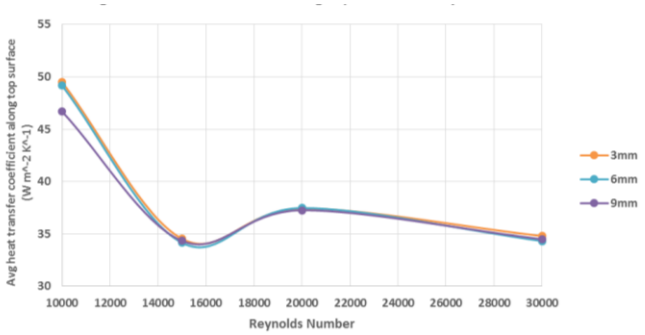

Chart -11: Average Wall Heat Transfer Coefficient along Top Surface Vs Reynolds Number

3.6.2 Bottom Surface

Table -5: Average Wall Heat Transfer Coefficient along Bottom Surface

Reynolds Number	Rib Type	Average Wall Heat Transfer Coefficient (W m^-2K^-1)
10000	3mm	49.97
	6mm	49.67
	9mm	46.42
15000	3mm	34.44
	6mm	34.52
	9mm	34.32

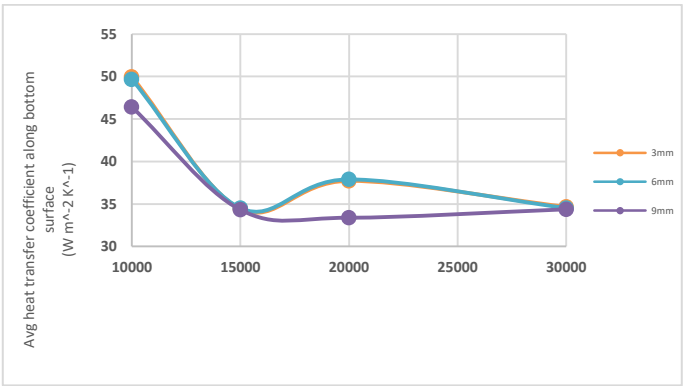

Chart -12: Average Wall Heat Transfer Coefficient along Bottom Surface Vs Reynolds Number

3.7 Variation of Pressure drop with Reynolds number

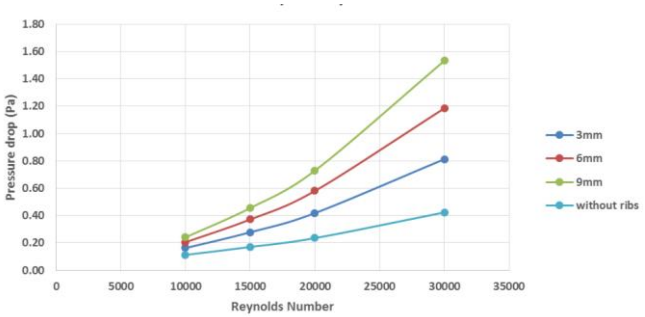

Chart -13: Pressure Drop Vs Reynolds Number

It is noticed that the pressure drop increases for each Reynolds number with increase in rib size.

3.8 Variation of Friction Factor with Reynolds number

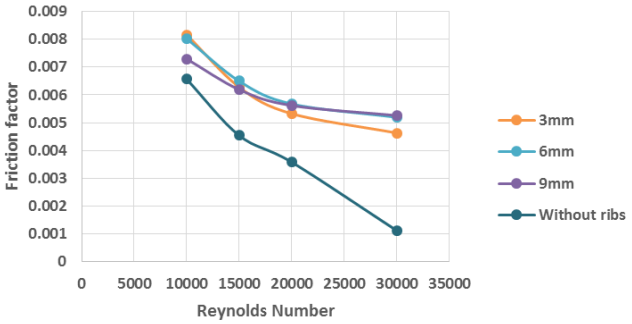

Chart -14: Friction Factor Vs Reynolds Number

4. CONCLUSION

Computational study has been carried out on rectangular channels with smooth channel and sharp boot shaped ribs of 3mm, 6 mm, and 9mm heights to get the optimum heat transfer for ribs using ANSYS 15 and the results are obtained. It is therefore observed that 6mm sharp boot ribbed channel produced maximum heat transfer rate in the channel for every Reynolds number. Further analysis study can be done

by changing the shape of the ribs like triangular shape, trapezium etc at different heights to find out the heat transfer rate. The analysis could also be carried out for some higher Reynolds number and also different orientation and aspect ratio of the ribs can be considered.

REFERENCES

[1] Kalapala P., Prasad, B.A., Anandarao, M., "Material Optimization and Dynamic Approach for performance criteria in application to Gas Turbine Blade to overcome resonance", International Journal of Scientific & Engineering Research, 8(6), 189-196, 2017.

[2] Win Lai Htwe, Htay Htay Win, Nyein Aye San, "Design And Thermal Analysis Of Gas Turbine Blade", International Journal of Mechanical And Production Engineering, 62-66, Volume- 3, Issue-7, July 2015.

[3] Ahmed Abdulhussein Jabbar1, A. K. Rai2, P. Ravinder Reedy3 & Mahmood Hasan Dakhil, "Design And Analysis Of Gas Turbine Rotor Blade Using Finite Element Method", International Journal of Mechanical and Production Engineering Research and Development , 73-94, Vol. 4, Issue 1, Feb 2014.

[4] V. Vijaya Kumar, R. Lalitha Narayana, Ch. Srinivas, "Design and Analysis of Gas Turbine Blade by Potential Flow Approach", Int. Journal of Engineering Research and Applications, 187-192, Vol. 4, Issue 1(Version 1), January 2014.

[5] G D Ujade, M B Bhambere, "Review Of Structural And Thermal Analysis Of Gas Turbine Blade", Int. J. Mech. Eng. & Rob. Res, 347-352, Vol. 3, No. 2, April 2014.

[6] Prasad R D V, G Narasa Raju , M S S Srinivasa Rao , N Vasudeva Rao,"Study State Thermal and Structural Analysis of Gas Turbine Blade Cooling System", International Journal of Engineering Research & Technology (IJERT), 1-6,Vol. 2, No. 1, January 2013.

[7] Nithin Kumar K C, Tushar Tandon, Praveen Silori, Amir Shaikh, "Structural Design and Analysis of Gas Turbine blade using CAE tools", International Journal of Engineering Research & Technology, 469-474, Vol. 3 Issue 10, October 2014.

[8] Sulaiman, K.S., Rameshkumar, G.R., "Vibration Diagnosis Approach for Industrial Gas Turbine and Failure Analysis", British Journal of Applied Science & Technology, 14(2), 1- 9, June 2016.

[9] Mohamad, B.A., Abdelhussien, A., "Failure Analysis of Gas Turbine Blade Using Finite Element Analysis", International Journal of Mechanical Engineering and Technology (IJMET) 7(3), 299-305, 2016.

[10] Abdul Qadir Talal, Dr K Fazlur Rahman, "Design and Analysis of a Gas Turbine Blade", International Research Journal of Engineering and Technology, 479-486, Volume: 07 Issue: 11 , Nov 2020.